Investigating Asphaltene Deposition Kinetics through Particle Size and Count Correlation

Muhammad Ali * and Alake Adedamola Stephen

Posted Date: 25 September 2023

doi: 10.20944/preprints202309.1646.v1

Keywords: Asphaltene kinetics, aggregate kinetics, precipitation kinetics

Article

Investigating Asphaltene Deposition Kinetics through Particle Size and Count Correlation

Muhammad Ali Buriro * and Alake Adedamola Stephen

Geosciences and Geological Engineering and Petroleum Engineering Department, Missouri University of Science and Technology, Rolla, Missouri, 65401 United States.

* Correspondence: maf2z@mst.edu (Muhammad Ali)

Abstract: Asphaltene precipitation and deposition pose significant operational challenges in both reservoirs and surface facilities by inducing formation damage. To understand the kinetics involved in asphaltene particle nucleation, growth, and aggregation, this study employed confocal microscopy and centrifuge-based methods under a unified set of experimental parameters. The acquired time-resolved particle size images were analyzed using MIPAR image processing software, while asphaltene mass yield was quantitatively evaluated through centrifugation. Experimental conditions were varied to study the effects of heptane concentration, asphaltene concentration, and shear rate. Notably, this investigation introduces, for the first time, the parameter of particle count as an additional variable influencing asphaltene mass production. This study aims to discern how particle count correlates with asphaltene mass yield over time. Results indicate that the minimum mean particle diameter was observed to be 2 microns, which progressively grew up to 80 microns. The mean particle diameter exhibited a positive correlation with both asphaltene concentration and shear rate, whereas an inverse correlation was seen with heptane concentration. Furthermore, the asphaltene mass yield was found to increase with greater asphaltene and heptane concentrations, as well as with higher shear rates. The relationship between mean particle diameter and mass yield was found to be nonlinear. In the early stages, a higher prevalence of small particles contributed to a greater total particle count, while at later stages, particle aggregation led to the formation of larger particles that influenced the overall asphaltene mass. The insights gained from understanding the relationship between particle diameter, count, and mass yield are crucial for advancing the fundamental science of asphaltene precipitation and deposition. These findings may also guide future research that relies solely on particle counts for assessing asphaltene deposition.

Keywords: asphaltene kinetics; aggregate kinetics; precipitation kinetics

1. Introduction

Asphaltenes are complex fractions within petroleum fluids that exhibit variations in molecular weight, structure, and polarity (Speight., 2014). These fractions are notably soluble in aromatic solvents such as toluene but insoluble in alkanes like n-hexane, classifying them as a distinct solubility class (Yarranton and Masliyah., 1996; Elturki and Imqam., 2020). Their significance in reservoir operations is evident from their tendency to deposit on rock surfaces, thereby causing potential formation damage (Moghanloo et al., 2018). This deposition process occurs through three sequential stages: precipitation, flocculation, and surface deposition (Yi et al., 2009). The precipitation stage entails the formation of distinct phases due to thermodynamic equilibrium, influenced by variables such as pressure, temperature, or reservoir composition (Naghiem et al., 1998; Buriro and Muhannad, 2013). Under ambient conditions, these particles can reach sizes up to 1 μm (Kempkes et al., 2008). Subsequently, the particles undergo flocculation, leading to particle sizes greater than 1 μm (Khanifar et al., 2013; Shafiee, 2014). Various studies have explored the kinetics of asphaltene aggregation, focusing on either particle size or yield percentage but seldom both under uniform conditions (Rastegari et al., 2004; Ashoori et al., 2005; Maqbool et al., 2011). For example, Rastegari et al. (2004) analyzed asphaltene particle growth in toluene solutions, examining the role of shear rate, asphaltene concentration, and temperature. Their findings suggested three distinct growth regions and reversible flocculation patterns. Ashoori et al. (2005) explored aggregation

 doi:10.20944/preprints202309.1646.v1

kinetics in toluene-heptane mixtures, identifying diffusion-limited and reaction-limited aggregation mechanisms. They noted that critical micelle concentration for asphaltenes is around 3g/l, above which the diffusion-limited aggregation dominates.Similarly, Maqbool et al. (2011) focused on the time dependency of asphaltene precipitation from crude oils. They found that the time to reach equilibrium and maximum yield percentages differed based on the concentration of the n-alkane precipitant used. Alberto, J. (2020) extended this work to multiple crude oils and measured asphaltene yields and particle sizes through gravimetry and microscopy, respectively.Despite these efforts, no study has yet integrated particle size and yield percent analysis under uniform conditions. Furthermore, the relationship between particle size, asphaltene yield, and particle count remains unexplored, representing a significant gap in the existing literature.

In this work, the kinetics of asphaltene particle growth and yield percentage were investigated under identical conditions using asphaltene-toluene mixtures. Western Missouri Heavy oil served as the source for extracting asphaltene particles. A liquid mixture of asphaltene-toluene with varying asphaltene concentrations was prepared to enable particle-size characterization. High-resolution confocal microscopy and image processing software (MIPAR) were utilized for particle size analysis, and centrifuge-based experiments were conducted to determine asphaltene yield percentages. Both particle size and yield experiments were performed under the same conditions, taking into account variables such as shear rate, asphaltene weight content, and the ratio of heptane to toluene. This investigation aimed to fill existing gaps in the literature and contribute to the growing body of knowledge required for effective reservoir management strategies against asphaltene-related formation damage.

2. MATERIAL AND METHODOLOGY

2.1. Crude oil sample and properties

In this investigation, a crude oil sample was taken from the South-west Missouri-Kansas Border in the United States of America and utilized to extract asphaltene. The API Gravity, Viscosity, and Asphaltene Content were determined in the lab. To determine the amount of asphaltene in the sample, the IP-143 method was utilized (Andersen and Birdl, 1990). API gravity was measured using a hydrometer. The viscosity was determined using a Brookfield DV2T Touch Screen Viscometer. The measured findings are shown in Table 1

Table 1. Crude Oil Properties

Property	Result
API	17
Viscosity	6000-9000 cp
Asphaltene Content	14.8 wt.%

2.2. Materials used in this study

Table 2 provides an overview of the molecular weights, purity levels, and suppliers of all the chemicals and materials utilized in the research. No additional processing or purification was performed on the chemical additives. Toluene, having a refractive index of 1.4969, was employed as the solvent, whereas n-heptane with a refractive index of 1.3888 served to trigger asphaltene precipitation as the precipitating agent.

Preprints (www.preprints.org) | NOT PEER-REVIEWED | Posted: 25 September 2023 doi:10.20944/preprints202309.1646.v1

Table 2. Materials utilized in this study.

Chemical	Chemical Formula	MW(g/mol)	Purity	Supplier
Heptane	C_7H_{16}	100.21	≥ 99%	Lab Alley Powering Science
Toluene	C_7H_8	92.14	≥ 99%	Fisher Scientific
Crude Oil	-	-	-	Western Missouri Oil Field
Frosted Microscopic Slides	-	-	-	Karter Scientific
Cover lids (24mm x 50mm)				Karter Scientific
Whatman 10-micron filter paper	-	-	-	OFITE, Inc Filter paper

2.3. Asphaltene Extraction Experimental Procedure

As illustrated in Figure 2, a specialized closed-chamber filtration apparatus was designed for asphaltene particle extraction. To initiate the procedure, a 22-micron Whatman filter paper was positioned in the apparatus, and its baseline weight was documented. In a subsequent step, 1 gram of crude oil was amalgamated with 40 cm^3 of heptane in a glass beaker. This mixture was then subjected to mechanical stirring at a rate of 200 rpm for a period of 60 minutes, facilitated by a magnetic stirrer. To mitigate the evaporation of heptane, the beaker was securely capped. Following agitation, the prepared sample was transferred to the filtration apparatus, which was hermetically sealed. The sample was allowed to undergo filtration for a 24-hour period. After this interval, the filter paper, now laden with asphaltene particles, was carefully removed (see Figure 3a) and exposed to open-air conditions for an additional 24 hours to achieve complete drying (see Figure 3b). The weight percentage of the extracted asphaltenes was subsequently determined according to Equation 1.

$$\text{Asphaltene wt.\%} = \frac{\mathrm{w_{wet}} - \mathrm{w_{dry}}}{\mathrm{A_t}} \quad \mathbf{1}$$

Where w_{dry} is the weight of filter paper before filtration, w_{wet} is the weight of filter paper after filtration and A_t is the total weight of asphaltic crude oil.

 doi:10.20944/preprints202309.1646.v1

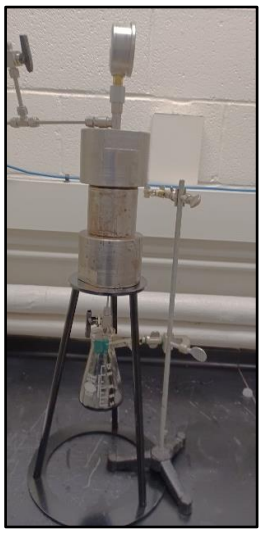

Figure 1. Filtration Apparatus used for Asphaltene Extraction.

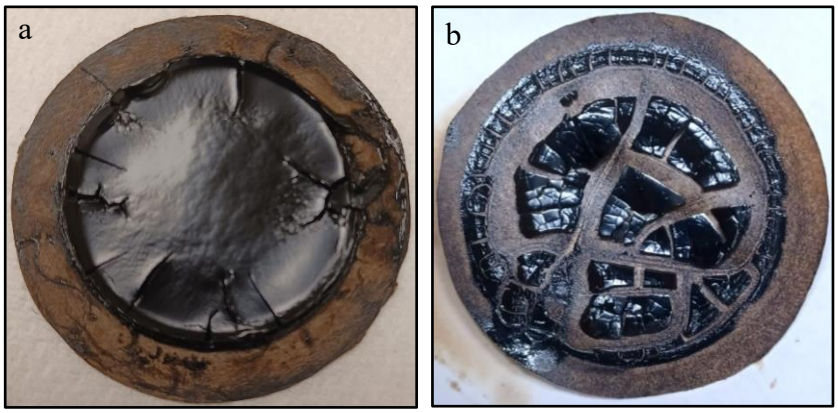

Figure 2. Asphaltene Precipitation on Filter Paper (a) before drying, (b) after 24hrs.

The following calculation was done to obtain asphaltene weight percent (see Equation 1):

$$\text{Asphaltene wt.\%} = \frac{\mathrm{W_{wet} - W_{dry}}}{\mathrm{A_t}} \quad \mathbf{1}$$

Where w_{dry} is the weight of filter paper before filtration, w_{wet} is the weight of filter paper after filtration and A_t is the total weight of asphaltic crude oil.

2.4. Asphaltene-Toluene mixture preparation

Table 3 details the concentrations of asphaltene particles that were solubilized in 10 cm^3 of toluene, with all tests conducted at a stable temperature of 25°C. After the initial mixing, each sample underwent a 120-minute sonication treatment and was subsequently left to settle overnight. Post this 24-hour settling period, confocal laser microscopy was employed to validate the complete dissolution of the asphaltene particles in the toluene medium. It is pertinent to note that at elevated concentrations of asphaltenes in the modeled systems and in heptane-diluted bitumen, the fluid became too opaque for accurate particle measurement. Similarly, at asphaltene concentrations falling below 0.05 kg/m^3, the scarcity of particles rendered the analysis unreliable. As a result, the scope of the experiments was restricted to a well-defined range of asphaltene concentrations, specifically between 0.05 kg/m^3 and 0.1 kg/m^3.

Preprints (www.preprints.org) | NOT PEER-REVIEWED | Posted: 25 September 2023 doi:10.20944/preprints202309.1646.v1

Table 3. Concentrations of Asphaltene-Toluene Mixtures Utilized in the Study

Prepared Sample	Toluene	Asphaltene
10 gram per liter	10 cm^3	0.1 g
8 gram per liter	10 cm^3	0.08 g
5 gram / liter	10 cm^3	0.05 g

2.5. Particle Size Analysis using Confocal Microscopy

Particle-size distribution of asphaltenes was determined using Nikon Confocal Microscopy with a 10x objective lens, facilitating the study of particles ranging from 0.5 µm to 150 µm. Utilization of a green laser and the Time-Domain (TD) scanner option was implemented to enhance the investigation. Upon initiating the experimental sequence, heptane was added to the asphaltene-toluene mixture, which was then mildly agitated prior to its transfer into a cuvette for detailed analysis. Time-series measurements were conducted at intervals including 5, 15, 30, 45, 60, 75, 90, 120, 150, 180, 240, and 300 minutes. A small volume of the prepared mixture was dispensed onto a microscopic slide, immediately sealed with a cover slip, and subjected to confocal microscopy. The laser of the particle-size analyzer was programmed to focus on a confined area within the cuvette; therefore, to ensure a representative dataset, additional images were captured at five different locations across the slide. Data interpretation was carried out using MIPAR image processing software.

This experimental framework was devised to evaluate the influence of key parameters—namely, heptane concentration, asphaltene concentration, and shear rate—on the size distribution of asphaltene particles (details can be found in Table 4). In this nomenclature, "X:Y Heptol" refers to a heptane:toluene solution where X and Y correspond to the volume fractions of heptane and toluene, respectively. The methodology was aligned with previous work conducted by Rastegari H. et al. (2004). To generate a specified shear rate, a viscometer equipped with a 63 spindle was employed, operating at 100 rpm.

Table 4. Experimental Procedure for Particle Size Analysis

Effect of Heptane Concentration			
Heptol Concentration	Temperature	Asphaltene Content	Shear Rate
60:40	25 °C	10 g/L	0 1/s
70:30	25 °C	10 g/L	0 1/s
Effect of Shear Rate			
60:40	25 °C	10 g/L	0 1/s
60:40	25 °C	10 g/L	100 1/s
Effect of Asphaltene Concentration			
60:40	25 °C	10 g/L	0 1/s
60:40	25 °C	8 g/L	0 1/s

 doi:10.20944/preprints202309.1646.v1

60:40	25 °C	5 g/L	0 1/s

2.6. Image analysis of asphaltene particles

In this study, MIPAR image processing software was employed to analyze confocal laser microscopy images. Various image enhancement techniques were applied, including the expansion of pixel intensity range, median filtering, Gaussian noise filtering, and top-hat filtering. To capture a comprehensive range of particle sizes, an intensity threshold range from 100 to 190 Imax was utilized, supported by an optimization function. Particles with dimensions below 200 nm were excluded via area opening, and particles adjacent to image borders were masked to eliminate artifacts arising from the system's spatial resolution. The analytical scope focused on particles possessing a radius greater than 200 nm. MIPAR software subsequently calculated key metrics, such as mean equivalent diameter, mean minimum diameter, particle count, and average inter-particle distance, based on the refined binary images. To ensure a representative sample, five distinct images from various slide locations were analyzed to determine the mean particle diameter.

2.7. Procedure for Yield Percent Experiment

In accordance with the experimental methodology adopted from Maqbool et al. (2009), an LD-3 Electronic Centrifuge was utilized to separate asphaltene precipitates from crude oil mixtures over specified time intervals. The centrifuge has a maximum operational speed of 4000 rpm, exerting a relative centrifugal force up to 1975g. A synthetic oil mixture of asphaltene and toluene, prepared as delineated in Section 4.4, served as the base fluid. Heptane was introduced at concentrations of 60:40 and 70:30 at ambient conditions to initiate the precipitation process. Time intervals for evaluating asphaltene precipitation included 5, 15, 30, 45, 60, 75, 90, 120, 180, 240, and 300 minutes. For each time interval, temperature-resistant centrifuge tubes were meticulously cleaned and pre-weighed. A 1.4 mL sample was extracted from the mixture via a syringe and then subjected to centrifugation at 4000 rpm. Upon completion, the tube was weighed again and left to dry in open air. This process was repeated for each time interval. After the experiment's conclusion, all tubes were placed in a vacuum oven set at 115°C for 24 hours to facilitate the evaporation of heptane (boiling point 98.42°C) and toluene (boiling point 110°C). The tubes were then re-weighed, accounting for residual asphaltene content. To assess any weight reduction in the tubes due to high-temperature exposure, three empty tubes were weighed and subjected to similar oven conditions. The fraction of precipitated asphaltene was calculated using a specific formula, which will be elaborated upon in subsequent sections.

2.8. Assumptions used in this work

1. Nucleation term is used when asphaltene particles came out of solution and form a minimum particle size of 2 microns.
2. Growth is termed as a continuous increase of particle size over time
3. Aggregation mechanism is referred to sudden increase in the mass yield for more than 6 mg.

3. Experimental Result and Discussion

In this section, the focus is directed towards analyzing the influence of key variables such as heptane concentration, asphaltene weight content, and shear rate on two primary metrics: the mean particle diameter of asphaltene and the yield percentage of precipitated asphaltene. Additionally, comparative insights are offered on particle count, asphaltene yield, and the range of particle sizes. The mean equivalent diameter serves as a conventional approach to aggregate classification. It is defined as the diameter of a circle possessing an aggregate sectional area equivalent to that of the particle, calculated using $d = 2\sqrt{\text{Area}/\pi}$. The yield percentage is quantified as the mass of the dried precipitate relative to the mass of asphaltenes present in the initial solution, expressed in percentage

 doi:10.20944/preprints202309.1646.v1

terms. The asphaltene particle size distribution range denotes the variance in the mean equivalent diameter of all flocs at each discrete time interval. For visual clarity, solid lines are incorporated in all graphical representations within this study.

3.1. Confocal images of Western Missouri oil

Figure 3a displays time-lapsed, processed confocal images for South-Western Missouri oil at a 5g/l asphaltene concentration, 60% heptane concentration, and 25°C. Initially, asphaltene flocs are observed within the 2 to 5-micron range. Post 90 minutes, the floc size expands dramatically, reaching up to 35 microns, but later contracts to a 2 to 20-micron range at the 300-minute mark. Figure 3b, keeping other parameters constant, highlights the processed images at 8g/l asphaltene concentration. At 5 minutes, the mean particle diameter varies between 2 to 18 microns. After 90 minutes, the particle size lies in the 2 to 30-micron range and extends up to 50 microns by 300 minutes. In Figure 3c, set at 10g/l, the initial particle size spans 2 to 8 microns, expanding to 22 microns at 90 minutes and 50 microns by 300 minutes. A noticeable increase in particle count over time is evident from Figure 3c. Figure 3d shows the processed image at 70 % heptane concentration, 10g/l asphaltene concentration, and 25 ^{O}C. the result indicates that at 5 minutes, the mean particle diameter is in the range of 2 to 15 micron. After the mean equivalent diameter increase from 3 to 36 microns while at 300 mean particle diameter increases from 3 to 60 microns. Figure 3e shows the processed image at a 100-rpm shearing rate with 10g/l asphaltene concentration, 60% heptane concentration, and 25 ^{O}C. The mean particle diameter range is between 2.5 to 11 microns at 5 minutes. After 90 minutes mean particle diameter increased and the range in between 4- and 55 microns. after 300 minutes, the mean asphaltene diameter range between 2 to 65 microns. Across all processed images, a consistent increase in particle count is also observed over time.

Preprints (www.preprints.org) | NOT PEER-REVIEWED | Posted: 25 September 2023 doi:10.20944/preprints202309.1646.v1

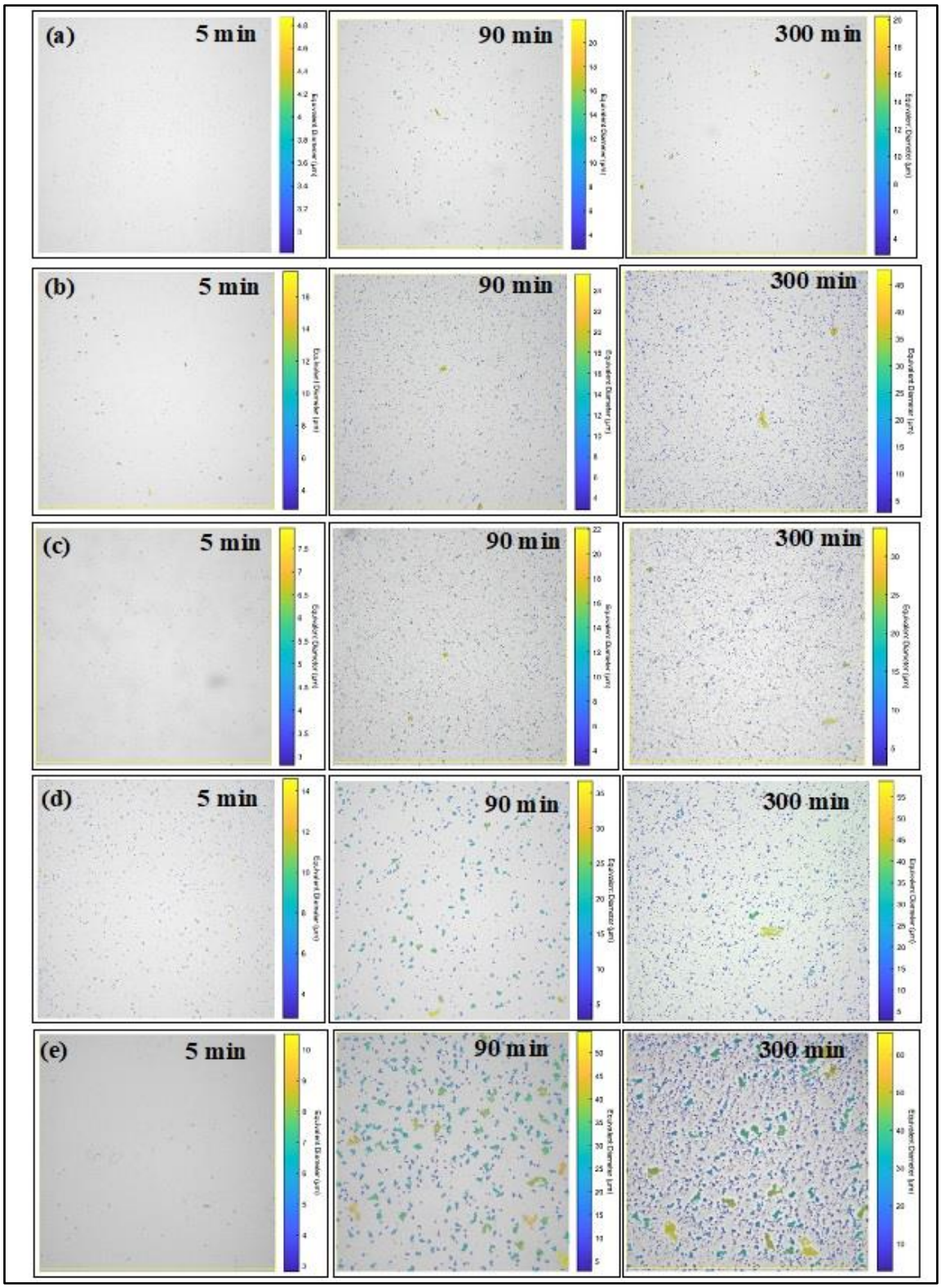

Figure 3. Processed images using MIPAR software (a) at asphaltene concentration 5g/l (b) at asphaltene concentration 8g/l, (c) at Asphaltene concentration 10g/l (d) 70:30 heptane to toluene ratio (e) 100 RPM shearing.

3.2. Particle Size Analysis using Confocal Microscopy

Results

 doi:10.20944/preprints202309.1646.v1

There are three points of interest. 1)initial diameter 2) Sharp increases or decrease in the particle diameter 3) stabilize particle diameter over long time. **Figure 4a** shows the effect of heptane concentration on mean equivalent diameter in 60:40 and 70:30 heptane to toluene ratios, referred to as (HEPTOL), at a concentration of 10 g/liter asphaltene and a temperature of 25 °C. The study lasted from 0 to 300 minutes. The results show that at a 60:40 HEPTOL ratio (Red line), initial mean particle size was 3.92 micron after 5 minutes and 4.4 micron at 15 minutes. However, after 15 minutes, the mean particle diameter drops to 3.5 micron and continues to fall until 60 minutes. The particle size increases dramatically after 60 minutes, reaching 7.7 micron at 90 minutes. After 90 minutes, the particle diameter stabilizes in the 7.3-to-7.4-micron range. Asphaltene particle size at 70:30 ratio (black line) is 3.5 micron after 5 minutes of heptane addition and reaches a high of 5.8 micron at 15 minutes. After 15 minutes, the mean particle diameter has continued to decrease till 45 minutes where particle diameter was 4 microns. The mean equivalent diameter ranges stabilized from 3.5 to 3.7 micron between 45 and 300 minutes. The result is in agreement with those of Duran et al., 2019.

Figure 4b shows the average equivalent diameter for all given asphaltene concentrations. Based on the results, the initial mean equivalent diameter recorded at 5 min was 3 microns at 5 g/L. The average equivalent diameter increased to 3.4 microns after 5 to 45 minutes. At 45 min, there was a sharp increase from 3.4 to 4.8 microns to 60 min. After 60 minutes, the average equivalent diameter decreased again to 3.7 microns and stabilized in the range of 3.7 to 4.5 microns from 90 to 300 minutes. At 8 g/L, the initial mean equivalent diameter recorded at 5 min was 3.6 microns. After 5 minutes, the diameter increased to 5.38 microns at 45 minutes. After 45 minutes, the diameter continued to drop to 3.78 microns until 90 minutes. After 90 minutes, the diameter increased to 6.2 microns after 240 minutes. Finally, a diameter of 5.48 was observed at 300 minutes**.** The mean starting particle size at 10 g/L (black line) was 3.92 microns at 5 minutes and 4.4 microns at 15 minutes. After 15 minutes, however, the average particle diameter reduces to 3.5 m and continues to decrease until 60 minutes. After 60 minutes, the particle size grows considerably, reaching 7.7 microns after 90 minutes. After 90 minutes, the particle diameter settles in the 7.3 to 7.4 m range. The result indicated initial and stabilized mean equivalent diameter increase with increase in the asphaltene concentration. The results are in agreement with Rastegari H. et al. (2004).

Figure 4c shows the mean equivalent diameter at different shear rates. Using no shear rate, was 3.92 microns at 5 minutes and 4.4 microns at 15 minutes. After 15 minutes, however, the average particle diameter reduces to 3.5 m and continues to decrease until 60 minutes. After 60 minutes, the particle size grows considerably, reaching 7.7 microns at 90 minutes. After 90 minutes, the particle diameter settles in the 7.3 to 7.4 m range. Using 100 rpm shear rate, the initial mean equivalent diameter of 4.3 was observed. After 5 minutes, the mean diameter reduces to 3.7 microns rill 30 minutes. A sharp increase in mean diameter of 11.59 micron starts at 30 minutes till 90 minutes. At 120 minutes the asphaltene mean diameter declines to 6.98 micron and stabilize in the range of 6.9 to 7.8 microns from 120 till 300 minutes. The results suggest that increasing the shear rate increases the mean asphaltene equivalent diameter. Higher initial mean diameter was also observed at 100 rpm. Results indicate the sharp increase in particle size is attributed to the aggregation mechanism. Furthermore, at 100 rpm, a faster and higher aggregation mechanism is observed then without shearing the synthetic oil. Therefore, Shearing the oil increases the asphaltene aggregation mechanism as well as reduces the aggregation time. The results are in agreement with Rastegari H. et al. (2004).

Discussion

Stabilized particle size at 60:40 is 7.3-7.4 micron while at 70:30 is 3.5 to 3.7. However, the total number of particles observed in 70:30 HEPTOL ratio are higher then 60:40 as shown in Figure 3-c and d. Heptane is a efficient precipitant of asphaltene, the better solubility of heptane in toluene-asphaltene system leads to reduced solubility of asphaltene that causes asphaltene particle to nucleate and grow that caused the higher mean equivalent diameter. At 70 % heptane concentration more asphaltene particle nucleate due to higher heptane concentration, however due to higher heptane ratio, the attraction forces between asphaltene-asphaltene particles monomers has reduced that has

Preprints (www.preprints.org) | NOT PEER-REVIEWED | Posted: 25 September 2023 doi:10.20944/preprints202309.1646.v1

caused reduced growth of particle size. Duran et al., 2019 has similar results where he indicated that the initial volume mean diameters and number counts both increased with increasing *n*-heptane content until reaching a plateau after reaching the plateau mean equivalent diameter decreases by increasing the Heptol ratio. A sharp increase in particle size starting at 75 minute at 60 % heptane concentration is due to the aggregation to asphaltene particles. The plausible explanation for aggregation is due to the high π−π stacking, van der Waals (vdW) interaction, hydrogen-bonding interaction, electrostatic (or ionic) interaction, polar−polar (dipole−dipole) interaction, mechanisms. (Keith et al., 2004; De León et al., 2014).

Figure 4b shows the mean equivalent diameter for different asphaltene concentrations. It depends on the required time for two asphaltene monomers to diffuse and reach to each other and the time that takes for particles to react with each other and form larger particles. Increasing the asphaltene concentration causes increasing the density of asphaltene. The average distance between asphaltene particle reduces as asphaltene particle concentration increases. This increases the collision and diffusion of micelles/ monomers causing the particle size to grow. (Anisimov et al.,1995; Soulgani et al., 2020). Furthermore, sharp incline at mean particle size for 10g/l attributed to higher aggregation was observed at 75 minutes. At 8g/liter, the smaller sharp incline was observed at 30 minutes then at 10 g/l. such sharp incline is also due to aggregation of the particles. It suggests that forces responsible for aggregation mechanism increases with the asphaltene concentrations. This result is in agreement with li et al., 2017; . As explained earlier the aggregation mechanism is caused by increased π−π stacking, van der Waals (vdW) interaction, hydrogen-bonding interaction, electrostatic (or ionic) interaction, polar−polar (dipole−dipole) interactions.

Figure 4c shows the mean equivalent diameter at different shear rates. The results suggest that increasing the shear rate increases the mean asphaltene equivalent diameter. This increase in mean equivalent diameter is due to better heptane-oil mixing, which reduces asphaltene solubility because heptane is a strong precipitant. In this work, a 63-number spindle with a viscometer was used, which results in better mixing but no particle breakage of asphaltene. However, there are several studies that show that increasing the shear rate reduces particle size. High rpm shearing or the device used (Magnetic stirrer in a small, confined space) may break the asphaltene particle, making it resoluble in asphaltene.

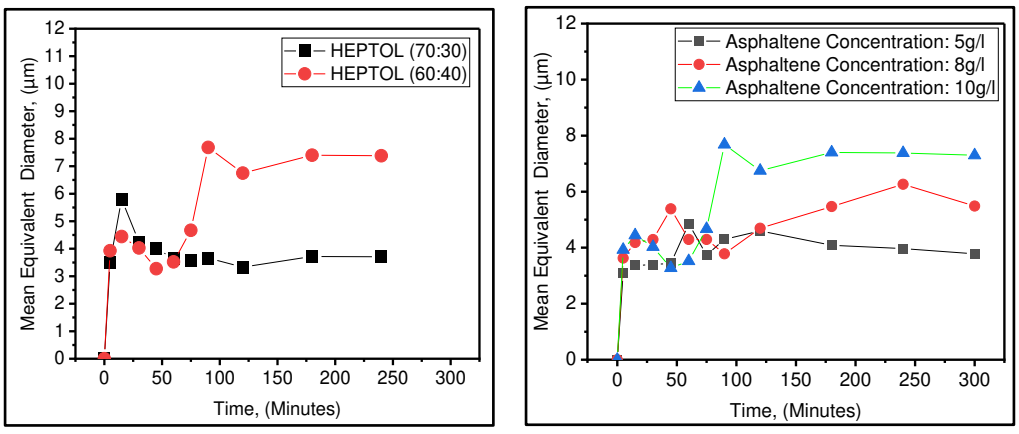

(**a**) (**b**)

Preprints (www.preprints.org) | NOT PEER-REVIEWED | Posted: 25 September 2023 doi:10.20944/preprints202309.1646.v1

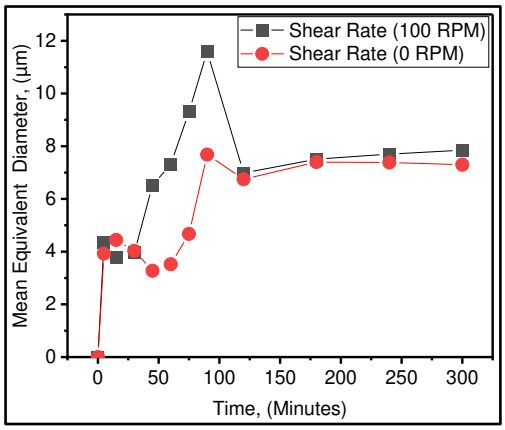

(c)

Figure 4. Asphaltene mean particle diameter over time (a) At different Heptane-Toluene concentration (b) At different asphaltene concentrations (c) At different shear rates.

3.3. Cumulative Yield Percent Analysis using Centrifuge Experiments

There are three points of interest in cumulative asphaltene yield results. 1) Rate of aggregation 2) Changes in rate of aggregation at different time steps. 3) Any sharp increase or decrease in cumulative asphaltene yield. 4) total asphaltene yield.

F**igure 5a** shows the effect of the asphaltene concentration on the cumulative asphaltene yield in 60:40 and 70:30 Heptol ratio. Using 70:30 Heptane ratio (red line), two zones are observed. Asphaltene yield grows linear from 0 min to 90 min at the rate of 0.42 mg per min in zone 1. However, the rate of aggregation declines at 0.242 mg per minute from 90 to 300 minutes in zone 2. No sharp increase in cumulative asphaltene yield was observed. At 60:40 ratio (black line), three different zones are observed. From 0 to 30 minutes, 0.33 mg per minute of rate of cumulative yield. A sharp increase is observed from 30 to 45 minutes. After 45 minutes till 300-minute, 0.23 mg per min is observed. Total asphaltene yield at 70:30 is 92.5 mg while 89 gram at 60:40 Heptane to toluene ratio out of total 100 grams in both cases. The result indicates that increasing the heptane to toluene ratio has increases the asphaltene precipitation yield. The results are in agreement with J.A Duran, 2019 and Maqbool et al 2009. The result indicates the two different regions of rate of cumulative asphaltene yield are observed. The trends are in good agreement with Maqbool et al 2008 at 46.5 vol% and 50 vol % of asphaltene. However. any sharp increase in cumulative yield is not observed in their results. In the first zone, the rate of asphaltene yield is higher than in zone two. This could be due to increase in heptane solubility while decreasing the asphaltene solubility leading to continuous nucleation of large number of particles in zone 1 and second zone nucleation of asphaltene particles decline considerably but large flocculates are formed due to aggregation mechanism as shown in Figure 3e. Therefore, zone 1 is dominated by nucleation of particles and zone 2 is dominated by aggregation of particles. The sharp increase at 60:40 at 90 minutes is attributed to the aggregation mechanism which is caused by high π−π stacking, van der Waals (vdW) interaction, hydrogen-bonding interaction.

Table 5. Effect of HEPTOL on asphaltene mass yield

Parameter: HEPTOL	Rate of cumulative yield in Zone 1 (mg/min)	Rate of cumulative yield in Zone 2 (mg/min)	Total Cumulative Asphaltene Yield (mg)
60:40	0.33	0.23	89

Preprints (www.preprints.org) | NOT PEER-REVIEWED | Posted: 25 September 2023 doi:10.20944/preprints202309.1646.v1

70:30	0.42	0.242	92.5

Table 6. Effect of shearing rate on asphaltene mass yield

Parameter: Shearing Rate	Rate of cumulative yield in Zone 1 (mg/min)	Rate of cumulative yield in Zone 2 (mg/min)	Total Cumulative Asphaltene Yield
No Shearing	0.33	0.23	89
100 RPM	0.33	0.24	91

Table 7. Effect of asphaltene concentration on asphaltene mass yield

Parameter: Asphaltene concentration	Rate of cumulative yield in Zone 1 (mg/min)	Rate of cumulative yield in Zone 2 (mg/min)	Total Cumulative Asphaltene Yield
10g/liter	0.33	0.23	89
8 g/liter	0.293	0.12381	70.5
5 g/liter	0.34	0.045238	40

Figure 5b shows the mean equivalent diameter for all given asphaltene concentrations at 23 C, no shearing and 60:40 heptane to toluene ratio. At 10g/liter (black line), three different zones are observed. From 0 to 30 minutes, 0.33 mg per minute of rate of cumulative yield. A sharp increase is observed from 30 to 45 minutes. After 45 minutes till 300-minute, 0.23 mg per min is observed. At 8 g/liter, three different zones are observed. From 0 till 75 minutes, the rate of cumulate yield is 0.293 mg per minute is observed. In zone two, A sharp increase in the yield is observed from 22 mg to 44.5 mg and in zone 3, from 90 min to 300 min, rate of cumulative yield of 0.12381 mg per min is observed. At 5g/liter asphaltene concentration, two zone are observed, in zone 1 from 0 to 90 min, the rate of cumulative yield is 0.34 mg per min. and in zone 2 from 90 to 300 minutes the rate of cumulative yield is 0.045238 mg per min. The result indicates the increasing the asphaltene concentration increases the cumulative asphaltene yield. The results are in good agreement with Rastegari H. et al. (2004). Furthermore, at 10g/liter and 8g/liter, a sharp incline is observed attributed to aggregation mechanism. However, such aggregation process starts earlier in the 10g/liter cases and later in 8 g/liter and at 5g/ liter no such aggregation process is observed. This indicates the increasing the asphaltene concentration causes quicker aggregation process and higher aggregation process. Furthermore, higher cumulative yield rate is attributed in zone 1 is attributed to higher nucleation and in zone 2m nucleation rate is reduced and aggregation of asphaltene flocs is increased. This implies that in zone 1 decreasing asphaltene solubility is the main mechanism while in zone 2 $\pi-\pi$ stacking, van der Waals (vdW) interaction, hydrogen-bonding interaction are dominant forces since no new asphaltene flocs are formed. **Figure 5c** shows the cumulative asphaltene yield at different shear rates. At no shearing (black line), as mentioned in earlier cases, three different zones are observed. From 0 to 30 minutes, 0.33 mg per minute of rate of cumulative yield. A sharp increase is

Preprints (www.preprints.org) | NOT PEER-REVIEWED | Posted: 25 September 2023 doi:10.20944/preprints202309.1646.v1

observed from 30 to 45 minutes. After 45 minutes till 300-minute, 0.23 mg per min is observed. At shearing of 100 rpm, similar trend was observed till 75 minutes, and after 75 minutes a sudden increase in particle size is observed from 36 mg to 58 mg. After that rate of cumulative yield is 0.24 mg per min. The result indicate the increasing the shearing rate will increase the asphaltene yield, The results are in good agreement with Nguyen et al 2021. This is due to better solubility of heptane due to high shearing. The result further records that sharp increase in cumulative yield attributed to aggregation process was observed multiple time at 100 rpm shearing rate. It is reflected that shearing the asphaltene could increase the forces such as π−π stacking, van der Waals (vdW) interaction, hydrogen-bonding interaction leading to higher aggregation process.

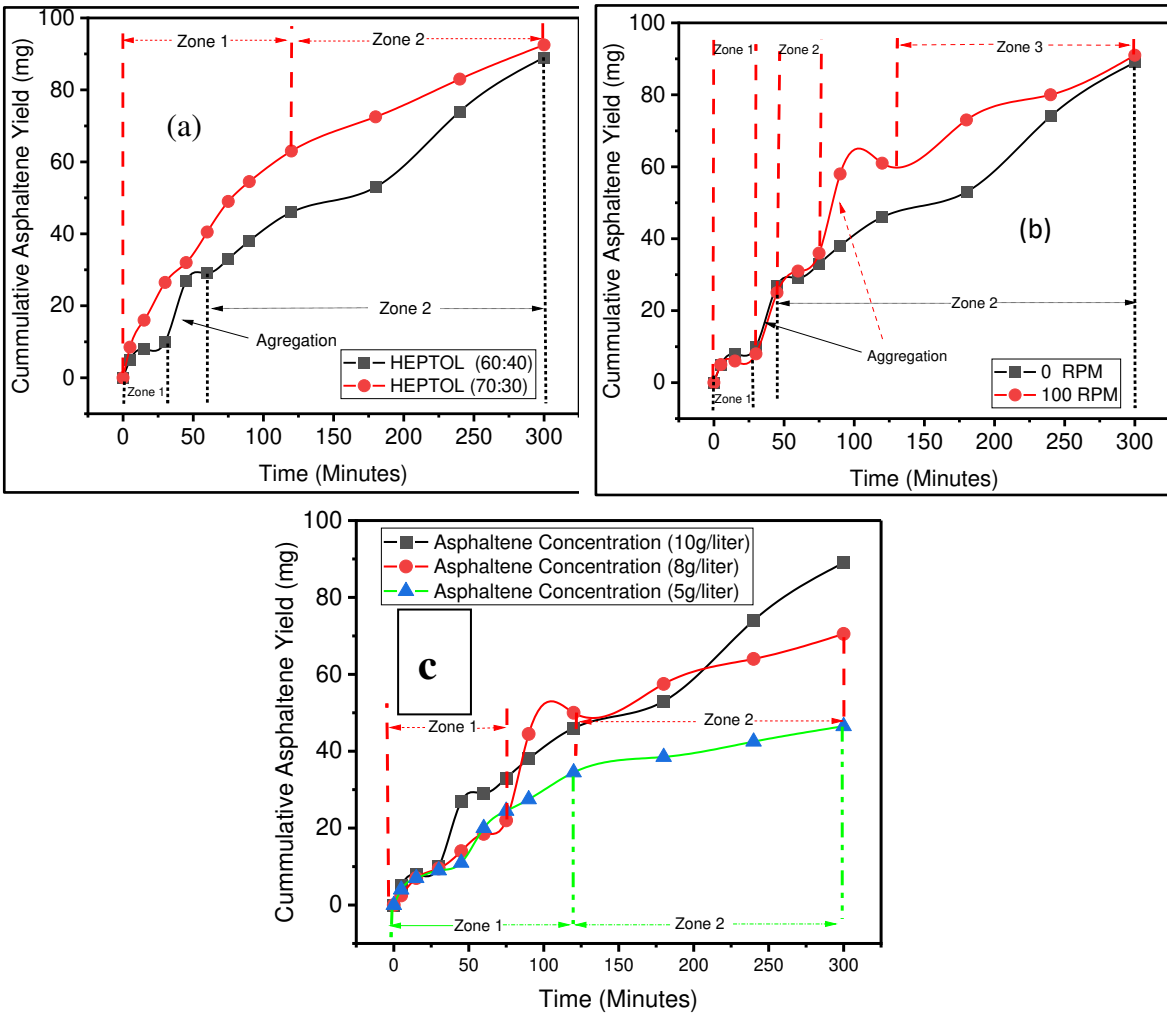

Figure 5. Cumulative asphaltene yield over time (a) At different Heptane-Toluene concentration (b) At different shear rates (c) At different asphaltene concentrations.

3.4. Correlation between asphaltene mass yield, asphaltene particle count and diameter range

In this study, the correlation between asphaltene mass yield, particle count, and diameter range is examined to address the existing gap in understanding the specific mass of asphaltene particles at various diameters. Given this gap, it's difficult to ascertain how the number of particles, based on their diameter, contributes to a specified mass yield. To tackle this, the study categorizes mean particle diameters into bins, each containing a range of mean equivalent diameters as detailed in Table 8. The study performs four distinct analyses: 1) comparing particle counts in early stages (0-90 minutes) to those in later stages (90-300 minutes) concerning mass yield; 2) focusing solely on early-stage particle counts in relation to mass yield; 3) examining particle counts only in later phases with respect to mass yield; and 4) observing overall trends in asphaltene mass yield over time.

 doi:10.20944/preprints202309.1646.v1

Figure 6a illustrates the time-dependent asphaltene yield and particle count at a concentration of 10g/l asphaltene, complemented by Table 8, which presents the particle size distribution for all experimental cases. The data suggest that asphaltene mass yield can fluctuate over time, influenced by various factors. For instance, the mass yield was initially 5 mg at 5 minutes, decreased to 2 mg at 60 minutes, escalated to 21 mg at 240 minutes, and then declined to 15 mg at 300 minutes. It's noteworthy that an identical mass yield of 5 mg was observed at both 5 and 90 minutes; however, the particle counts were 1149 and 755, respectively. At the 5-minute mark, the mass is predominantly made up of larger, recently nucleated particles ranging from 2 to 9 microns in diameter, while at 90 minutes, particles had diameters ranging from 2 to 30 microns, as detailed in Table 8. At the 120- and 180-minute intervals, the mass yields were 8 mg and 7 mg with particle counts of 1647 and 1560, respectively, indicating minimal fluctuation in particle numbers. Conversely, in an earlier timeframe between 15 and 30 minutes, particle counts were 996 and 626, with similar diameters. These findings suggest that early-stage processes are dominated by nucleation and aggregation, while later stages see growth and aggregation as the prevailing mechanisms, even though fewer particles are nucleating compared to the early stages.

At an asphaltene concentration of 8g/l, **Figure 6b** shows the time-resolved asphaltene yield and particle count. The data indicate that the asphaltene mass yield fluctuates between 2.5 to 4.5 mg and 5.5 to 7.5 mg from 120 to 300 minutes, echoing the previously established notion that mass yield can vary over time. At the early stage, marked at 45 minutes, the particle count is 1734 with a mass yield of 4.5 mg, while at the later stage, specifically at 120 minutes, the count is nearly identical at 1732 but with a slightly higher mass yield of 5.5 mg. In the early phase, smaller particles dominate, falling within a diameter range of 2-15 microns. In contrast, the later stage displays a variety of processes—nucleation, growth, and aggregation—with particle diameters ranging from 2 to 19 microns. Moreover, particle counts of 259 and 411 were observed at 5 and 30 minutes, both correlating to a mass yield of 2.5 mg. This behavior aligns with the earlier case, reaffirming that the early stage is largely governed by nucleation events, characterized by a smaller mean equivalent diameter

Figure 6c illustrates the asphaltene mass yield and particle count at an asphaltene concentration of 5g/l. The data reveal that mass yield ranges from 2-4 mg during the initial 0-45 minutes and spikes to 9 mg at 60 minutes, while between 75 and 300 minutes, it stabilizes within the 3-4.5 mg range, reaching 7 mg at 120 minutes. Despite the time lapse, the mass yield does not show a significant increase, although evidence of severe particle aggregation is observed in both early and late stages. The particle size predominantly falls between 2 to 11 microns across these stages. Notably, nucleation persists even in later stages at 120 and 180 minutes, where particle diameters of 3-5 microns prevail, as detailed in Table 8, pointing to the dominance of nucleation and aggregation mechanisms.

Turning to **Figure 6d**, which focuses on a heptane concentration of 70, the asphaltene mass yield varies from 5.5 to 10.5 mg in the early stage (0-90 minutes) but then increases to range between 8.5 and 10.5 mg. This pattern contrasts with previous observations. Specifically, at 5 and 120 minutes, the mass yield stabilizes at 8.5 mg with particle counts of 1977 and 2809, respectively. Similarly, at 30 and 240 minutes, a mass yield of 10.5 mg is coupled with particle counts of 2185 and 3500, respectively. These observations suggest that nucleation not only dominates the early stage but also intensifies in the later stage, co-occurring with particle growth.

Preprints (www.preprints.org) | NOT PEER-REVIEWED | Posted: 25 September 2023 doi:10.20944/preprints202309.1646.v1

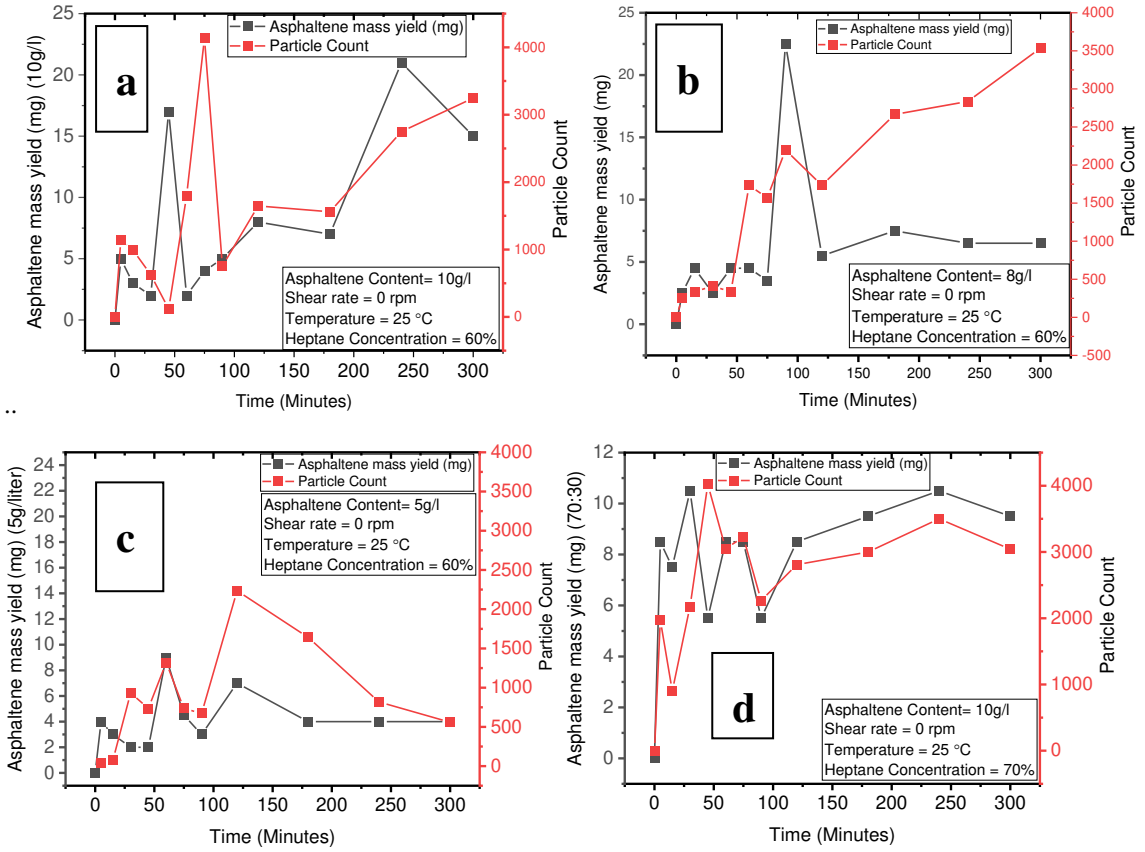

Figure 6. Asphaltene mass yield (mg) vs time, vs particle count (a) 10g/l, 25 ° C, 60 % heptane concentration and no shearing (b) 8g/l, 25 ° C, 60 % heptane concentration and no shearing (c) 5g/l, 25 ° C, 60 % heptane concentration and no shearing (d) 10g/l, 25 ° C, 70 % heptane concentration and no shearing.

Table 8. Asphaltene particle size distribution over time.

Bins	Counts										
(a) Asphaltene concentration 8g/liter, 25 °C,											
Particle Diameter Bin	5 mins	15 mins	30 mins	45 mins	60 mins	75 mins	90 mins	120 mins	180 mins	240 mins	300 mins
Total Counts											
3-5	230	242	265	974	1134	1134	1705	1024	1089	1124	2167
5-7	7	29	71	221	196	196	312	317	760	820	720
7-9	7	34	56	240	120	120	135	249	621	516	461
9-11	5	25	13	111	46	46	31	84	116	316	116
11-13	3	3	5	86	31	31	12	36	51	51	55
13-15	4	0	1	44	20	20	1	17	25	4	12
15-17	2	1		31	12	12	0	3	3	3	3
>> 17-19	1			25	10	10	2	4	1	1	1
(b) Asphaltene concentration5g/liter, 25 °C,											
Particle Diameter Bin	5 mins	15 mins	30 mins	45 mins	60 mins	75 mins	90 mins	120 mins	180 mins	240 mins	300 mins
Total Counts											

Preprints (www.preprints.org) | NOT PEER-REVIEWED | Posted: 25 September 2023 doi:10.20944/preprints202309.1646.v1

3-5	33	70	826	643	1081	643	431	1411	1131	583	446
5-7	2	4	70	67	128	67	126	368	281	144	81
7-9	0	1	29	19	72	19	89	272	174	70	24
9-11		0	4	3	16	3	16	95	44	14	4
11-13		1	2	0	10	0	3	50	7	6	0
13-15		1	0	2	7	2	3	18	3	0	0
15-17			1	0	1		3	12	1		0
>> 17-30			1		5		1	9			2
>>30-40								1			
>40-50				1		2		1			
>50+						1					
(c) Asphaltene concentration 10g/liter, 25 °C,											
Particle Diameter Bin	5 mins	15 mins	30 mins	45 mins	60 mins	75 mins	90 mins	120 mins	180 mins	240 mins	300 mins
Total Counts		996									
3-5	840	697	440	105	1508	2780	264	626		273	1928
5-7	174	173	99	8	180	497	109	279		131	480
7-9	107	101	71	5	76	410	118	279		128	466
9-11	17	17	12	0	17	166	71	154		43	187
11-13	7	3	4	0	6	123	57	113		36	119
13-15	1	2	0		1	65	38	78		24	48
15-17	3	3	0			48	36	52		16	27
>> 17-30						19	20			27	20
>>30-40						1				1	
>40-50										1	
>50+											1
(d) Asphaltene concentration 10g/liter, 70:30 HEPTOL Ratio , 25 °C, No shearing											
Particle Diameter Bin	5 mins	15 mins	30 mins	45 mins	60 mins	75 mins	90 mins	120 mins	180 mins	240 mins	300 mins
Total counts											
2.5	7	1285	1690	1690	3309	2737	1986	1986	2651	2668	7323
2.5-7.5	2	376	422	422	616	270	268	268	155	298	989
7.5-12.5		204	57	57	84	37	8	8	3	28	142
12.5-17.5		81	6		6	7	1	1	0	1	25
22.5		19	3		2	0	2	2		1	6
27.5		9			0	1	0			1	2
27.5 - 50		3			2	1				1	2

4. Conclusion

The mean asphaltene equivalent diameter in heptane-toluene-asphaltene solution begins at 2 microns and gradually increases to 80 microns. The mean particle diameter increases with increasing asphaltene concentration and shearing rate, whereas the mean particle size decreases with increasing heptane concentration, but the total number of particles increases significantly. Furthermore, a sudden sharp increase in particle size was observed, which reflects the aggregation process, while a sudden decrease in particle size reflects the asphaltene particle breakage mechanism.

Furthermore, as the asphaltene concentration, shearing rate, and heptane concentration increased, so did the asphaltene mass yield. However, two major zones with different asphaltene mass yield rates were detected in the cumulative asphaltene mass yield experiment. Zone 1 has a higher asphaltene mass yield rate than zone 2. Furthermore, in some cases, a sudden sharp increase in yield was observed, which reflects the aggregation process. When the asphaltene mass yield was compared to the particle count, it was discovered that the mass yield did not increase linearly, but rather showed an increase and decrease pattern. At early stage, for the same mass yield, there was a higher proportion of low diameter particles, whereas later, for the same mass yield, there was a lower proportion of lower particle size but a greater proportion of larger size asphaltene particles. It is concluded that the nucleation of asphaltene particles is a continuous process; however, larger flocculates are only observed later in the process. The following are the work's conclusions:

1. The mechanisms of nucleation, growth, aggregation, and breakage are all active in all cases.
2. Nucleation is a continuous process that was observed up until the last experiment, as evidenced by particle size.
3. The mechanism of aggregation occurs most notably at high asphaltene concentrations.
4. Increasing the asphaltene concentration causes aggregation to occur more quickly and in greater quantities.
5. Increasing asphaltene concentration and shearing rate increased mean particle diameter, while increasing heptane concentration decreased mean particle diameter but increased the amount of small asphaltene particles observed.
6. Increasing the concentrations of asphaltene, heptane, and shear rate resulted in higher mass yield over time.
7. Asphaltene mass yield or particle count does not increase linearly over time, but growth and breakage mechanisms are observed concurrently.

5. Future Work

This work has established that particle counts are influenced by the asphaltene mass yield. Therefore, a mathematical correlation may be developed in future that can predict the asphaltene mass yield based on its particle size and total number of counts

References

Ashoori, S., Abedini, A., Saboorian, H., Nasheghi, K. Q., & Abedini, R. (2009). Mechanisms of Asphaltene Aggregation in Toluene and Heptane Mixtures. In *Journal of the Japan Petroleum Institute* (Vol. 52, Issue 5).

Al-Qattan, A., Blunt, M. J., Gharbi, O., Badamchizadeh, A., Al-Kanderi, J. M., Al-Jadi, M., Dashti, H. H., Chimmalgi, V., Bond, D. J., & Skoreyko, F. (2012). Evaluation of the effect of asphaltene deposition in the reservoir for the development of the Magwa Marrat reservoir. *Society of Petroleum Engineers - Kuwait International Petroleum Conference and Exhibition 2012, KIPCE 2012: People and Innovative Technologies to Unleash Challenging Hydrocarbon Resources*, *2*, 550–568. https://doi.org/10.2118/163331-ms

Anisimov, M. A., et al. "Asphaltene Aggregation in Hydrocarbon Solutions Studied by Photon Correlation Spectroscopy." *The Journal of Physical Chemistry*, vol. 99, no. 23, 1995, pp. 9576–9580., https://doi.org/10.1021/j100023a040.

Buriro, M.&Talib Shuker, M. (2013, May 19-22). Minimizing asphaltene precipitation in Malaysian reservoir [Paper presentation]. SPE Saudi Arabia Section Technical Symposium and Exhibition, Al-Khobar, Saudi Arabia. doi: https://doi.org/10.2118/168105-MS

Duran, J. A., Schoeggl, F. F., & Yarranton, H. W. (2019, July 25). *Kinetics of asphaltene precipitation/aggregation from diluted crude oil*. Fuel.

De León, Jennifer, Hoyos, Bibian, & Cañas-Marín, Wilson. (2015). Insights of asphaltene aggregation mechanism from molecular dynamics simulation. *DYNA*, *82*(189), 39-44. https://doi.org/10.15446/dyna.v82n189.41963

Elturki, M., & Imqam, A. (2020, July 20-22). High pressure-high temperature nitrogen interaction with crude oil and its impact on asphaltene deposition in nano shale pore structure: An experimental study (pp. 2830-2845). *Unconventional Resources Technology Conference* (URTeC).

Elturki, M., & Imqam, A. (2021, June 28). Analysis of nitrogen minimum miscibility pressure MMP and its impact on instability of asphaltene aggregates: An experimental study [Paper presentation]. *SPE Trinidad and Tobago Section Energy Resources Conference*, Trinidad and Tobago. https://doi.org/10.2118/200900-MS

Li, X., Guo, Y., Boek, E. S., & Guo, X. (2017). Experimental study on kinetics of Asphaltene Aggregation in a microcapillary. *Energy & Fuels*, *31*(9), 9006–9015. https://doi.org/10.1021/acs.energyfuels.7b01170

Ferworn, K.A.; Svrcek, W.Y.; Mehrotra, A.K. (1993). Measurement of Asphaltene Particle Size Distributions in Crude Oils Diluted with n-Heptane. Ind. Eng. Chem. Res., 32, 955-959

Hung, J., Castillo, J., & Reyes, A. (2005). Kinetics of asphaltene aggregation in toluene-heptane mixtures studied by confocal microscopy. *Energy and Fuels*, *19*(3), 898–904. https://doi.org/10.1021/ef0497208

Kempkes, M.; Eggers, J.; Mazzotti, M. (2008). Measurement of Particle Size and Shape by FBRM and in situ Microscopy. Chem. Eng. Sci., 63 (19), 4656-4675

Keith L. Gawrys & Peter K. Kilpatrick (2004) Asphaltene Aggregation: Techniques for Analysis, Instrumentation Science & Technology, 32:3, 247-253, DOI: 10.1081/CI-120030536

Khanifar, A., Demiral, B. M. R., Alian, S. S., & Drman, N. (2011). Study of asphaltene precipitation and deposition phenomenon. *2011 National Postgraduate Conference*, 1–6.

Moghanloo, R. G., Davudov, D., & Akita, E. (2018). *Chapter Six - Formation Damage by Organic Deposition* (B. Yuan & D. A. B. T.-F. D. D. I. O. R. Wood (eds.); pp. 243–273). Gulf Professional Publishing. https://doi.org/https://doi.org/10.1016/B978-0-12-813782-6.00006-3

Maqbool, T.; Balgoa, A.T.; Fogler, H.S. (2009). Revisiting Asphaltene Precipitation from Crude oils: A Case of Neglected Kinetic Effects. Energy Fuels, 23, 3681-3686

Mostowfi, F.; Indo, K.; Mullins, O.C.; McFarlane, R. (2009). Asphaltene Nanoaggregates Studied by Centrifugation. Energy Fuels, 23(3), 1194-1200

Nghiem, L. X., Coombe, D. A., & Farouq Ali, S. M. (1998). Compositional simulation of asphaltene deposition and plugging. *Proceedings - SPE Annual Technical Conference and Exhibition*, *1999-September*, 129–140. https://doi.org/10.2523/48996-ms

Rastegari, K., Svrcek, W. Y., & Yarranton, H. W. (2004). Kinetics of asphaltene flocculation. *Industrial and Engineering Chemistry Research*, *43*(21), 6861–6870. https://doi.org/10.1021/ie049594v

Shafiee, M. Kinetics of Asphaltene Precipitation and Flocculation from Diluted Bitumen. (2014). MSc. Thesis. University of Calgary.

Saidoun, M. (n.d.). *Investigations into Asphaltenes Destabilization, Aggregation and Deposition*. Fluid mechanics [physics.class-ph]. Université de Pau et des Pays de l'Adour, 2020. English. ⟨tel-03459429⟩ https://tel.archives-ouvertes.fr/tel-03459429

Seifried, C. M.; Crawshaw, J.; Boek, E.S. (2013). Kinetics of Asphaltene Aggregation in Crude Oil Studied by Confocal Laser-Scanning Microscopy. Energy Fuels, 27 (4), 1865-1872

Soulgani, B.S., Reisi, F. & Norouzi, F. Investigation into mechanisms and kinetics of asphaltene aggregation in toluene/*n*-hexane mixtures. *Pet. Sci.* **17,** 457–466 (2020). https://doi.org/10.1007/s12182-019-00383-3

Speight, J. G. (2016). Chapter 4 - Reservoir Fluids. In J. G. Speight (Ed.), *Introduction to Enhanced Recovery Methods for Heavy Oil and Tar Sands (Second Edition)* (Second Edition, pp. 123–175). Gulf Professional Publishing. https://doi.org/https://doi.org/10.1016/B978-0-12-849906-1.00004-7

Yarranton, H. W., & Masliyah, J. H. (1996). Molar Mass Distribution and Solubility Modeling of Asphaltenes. *AIChE Journal*, *42*(12), 3533–3543. https://doi.org/10.1002/aic.690421222

Yi, T., Fadili, A., Ibrahim, M., & Al-Matar, B. (2009). *SPE European Formation Damage Conference held in Scheveningen*.